

Received: 2019.04.08

Accepted: 2019.04.24

Published: 2019.05.29

Gambogic Acid Shows Anti-Proliferative Effects on Non-Small Cell Lung Cancer (NSCLC) Cells by Activating Reactive Oxygen Species (ROS)-Induced Endoplasmic Reticulum (ER) Stress-Mediated Apoptosis

Authors' Contribution:

Study Design A
Data Collection B
Statistical Analysis C
Data Interpretation D
Manuscript Preparation E
Literature Search F
Funds Collection G

ABCDEF G 1 **Minghua Zhu**
ACEF 2 **Yinfang Jiang**
ADF 1 **Hao Wu**
ADE 1 **Wei Shi**
ADE 1 **Guirong Lu**
ACD 1 **Degang Cong**
CDF 1 **Keyuan Liu**
ACD 1 **Shaohui Song**
ACF 3 **Jianming Ren**

1 Department of Cardiothoracic Surgery, The Affiliated Hospital of Hangzhou Normal University, Hangzhou, Zhejiang, P.R. China
2 Department of Cardiovascular Medicine, Hangzhou First People's Hospital, Hangzhou, Zhejiang, P.R. China
3 Department of Respiratory Medicine, Chun'an Second People's Hospital of Hangzhou City, Hangzhou, Zhejiang, P.R. China

Corresponding Author: Minghua Zhu, e-mail: doctor_zhu@zju.edu.cn

Source of support: 1. Zhejiang Traditional Chinese Medicine Research Fund Project (2019ZA092); 2. The Key Project of Hangzhou Health Science and Technology Plan (2018Z04); 3. The Key Project of Zhejiang Province Traditional Chinese Medicine Science and Technology Plan (2015ZZ007)

Background: Gambogic acid (AG) is believed to be a potent anti-cancer agent. ER (endoplasmic reticulum) stress-induced cell apoptosis was identified as one of the anti-proliferative mechanisms of several anti-cancer agents. In this study, we investigated the involvement of ER stress-induced apoptosis in the anti-proliferative effect of GA on NSCLC (non-small cell lung cancer) cells.





Material/Methods: GA at 0, 0.5, and 1.0 $\mu\text{mol/l}$ was used to treat A549 cells. We also used the ER stress-specific inhibitor 4-PBA (4-phenylbutyric acid) (1 $\mu\text{mol/l}$) to co-treat the cells incubated with GA. Cell viability was assessed by MTT (methyl thiazolyl tetrazolium) assay. Cell apoptosis was evaluated by MTT (methyl thiazolyl tetrazolium) assay. Intracellular ROS (reactive oxygen species) production was detected by DCFH-DA (2,7-dichloro-dihydrofluorescein diacetate) fluorescent staining. Western blotting was used to assess the expression and phosphorylation levels of protein.

Results: GA treatment significantly reduced cell viabilities of NSCLC cells in a concentration-dependent manner. GA treatment increased intracellular ROS level, expression levels of GRP (glucose-regulated protein) 78, CHOP (C/EBP-homologous protein), ATF (activating transcription factor) 6 and caspase 12, as well as the phosphorylation levels of PERK (protein kinase R-like ER kinase) and IRE (inositol-requiring enzyme) 1 α . Co-treatment of 4-PBA dramatically impaired the inhibitory effect of GA on cell viability. 4PBA co-treatment also decreased expression levels of GRP78, CHOP, ATF6, and caspase12, as well as the phosphorylation levels of PERK and IRE1 α , in GA-treated NSCLC cells, without affecting ROS levels.

Conclusions: GA inhibited NSCLC cell proliferation by inducing ROS-induced ER stress-mediated apoptosis of NSCLC cells.

MeSH Keywords: **Apoptosis • Carcinoma, Non-Small-Cell Lung • Endoplasmic Reticulum Stress**

Full-text PDF: <https://www.medscimonit.com/abstract/index/idArt/916835>

 1657   4  20



Background

Lung cancer is one of the most common malignant cancers of the respiratory system and it has high morbidity and mortality rates. As the major pathological type of lung cancer, non-small cell lung cancer (NSCLC) accounts for over 80% of lung cancers [1]. Complete surgical resection is still considered the most effective therapy for NSCLC. Novel anti-cancer drugs have been developed in recent decades, many of which originate from natural medicinal herbs [2].

In the last 2 decades, bio-active agents extracted from natural medical herbs, especially Chinese medical herbs, have been attracting researchers' attention due to their wide spectrum of pharmacological activities. Gambogic acid (GA), which is also referred as $C_{38}H_{44}O_8$, is one of the active pharmacological components of a medical herb named Gaboge Hanburyi. In Traditional Chinese Medicine, Gaboge Hanburyi has been used in clinical treatment of many diseases [3]. Recently, the potent anti-cancer effects of GA were identified against multiple human cancers, including liver cancer, ovarian cancer, and breast cancer [4–6]. However, the exact molecular mechanisms of GA's anti-cancer activity are complicated and remain unclear.

The endoplasmic reticulum (ER) an important cellular organelle with important roles in regulating fundamental intracellular activities such as protein modification and calcium signaling [7]. When encountering some physiological and pathological challenges, normal ER functions are impaired and ER stress is initiated. Previous investigations have indicated there are 3 major ERS-specific signaling pathways involved in apoptotic signaling, which are transduced by the ERS sensor proteins PERK, ATF6, and IRE1 [8]. These signals result in activation of the pre-apoptotic factor CHOP, leading to cell death [8]. As inducing apoptosis is believed as an effective strategy of inhibiting cancer cell proliferation, it is reasonable to speculate that ERS-mediated apoptosis is involved in the anti-cancer effects of GA.

In this investigation, we assessed the anti-proliferative effect of GA on the human NSCLC cell line. The involvement of ERS-mediated apoptosis signals was also studied using an ERS-specific inhibitor. The results of this study add to our understanding of the anti-cancer activity of GA and also provide novel evidence for possible application of GA in the clinical treatment of NSCLC.

Material and Methods

Cell culture and treatment

The human NSCLC cell line A549 was purchased from the Cell Bank of the Typical Preservation Committee of the Chinese

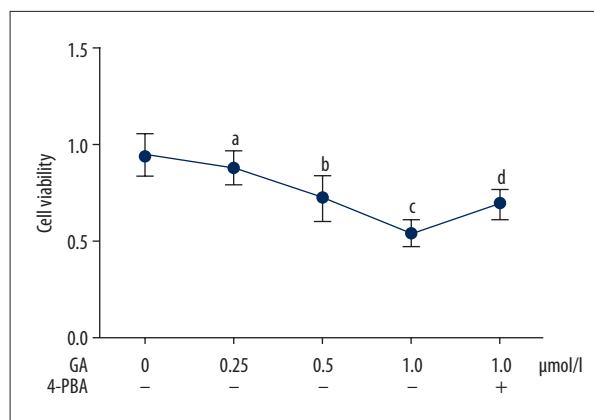


Figure 1. Figure shows the viabilities of A549 cells incubated with gambogic acid (GA) at concentrations of 0, 0.25, 0.5, and 1.0 $\mu\text{mol/l}$. Some cells incubated with GA at 1.0 $\mu\text{mol/l}$ were also co-treated with 4-PBA at a final concentration of 100 $\mu\text{mol/l}$. [^a Differences were statistically significant compared with control ($p < 0.05$); ^b Differences were statistically significant compared with cells incubated with GA at 0.25 $\mu\text{mol/l}$; ^c Differences were statistically significant compared with cells incubated with GA at 0.5 $\mu\text{mol/l}$; ^d Differences were statistically significant compared with cells incubated with GA at 1.0 $\mu\text{mol/l}$].

Academy of Science. Cells were cultured in Dulbecco's modified Eagle's medium (DMEM, Gibco) supplemented with 10% fetal bovine serum (FBS, Gibco) and an antibiotic mix (Sigma). Cells were maintained in a humidified incubator with 95% air and 5% CO_2 at 37°C. Cells were treated with GA (Sigma) at concentrations of 0, 0.25, 0.5, and 1.0 $\mu\text{mol/l}$ for 24 h. Some cells were pre-treated with ERS-specific inhibitor 4PBA at 100 $\mu\text{mol/l}$ for 2 h before GA incubation.

Cell viability evaluation

The cell viability was evaluated by colorimetric 3-(4,5-dimethylthiazol-2-yl)-2,5-diphenyltetrazolium bromide (MTT, Sigma) assay. Briefly, cells were seeded at 5×10^3 /well into a 48-well culture plate and maintained for 24 h. Cells were treated with GA and/or 4PBA and then washed with PBS and further incubated with MTT at a final concentration of 5 mg/ml for 4 h. DMSO (Sigma) was added into each well and the values of absorbance at 490 nm (A_{490}) was detected by a plate reader (Bio-Rad). Cell viability was then calculated according to the standard curve.

Intracellular ROS generation detection

ROS generated in the NSCLC cells was detected by 2,7-dichlorofluoresceindiacetate (DCFH-DA) fluorescent staining. Briefly, cells were incubated with 10 $\mu\text{mol/l}$ DCFH-DA (Sigma) at 37°C for 30 min to load the probes. Then, the fluorescence

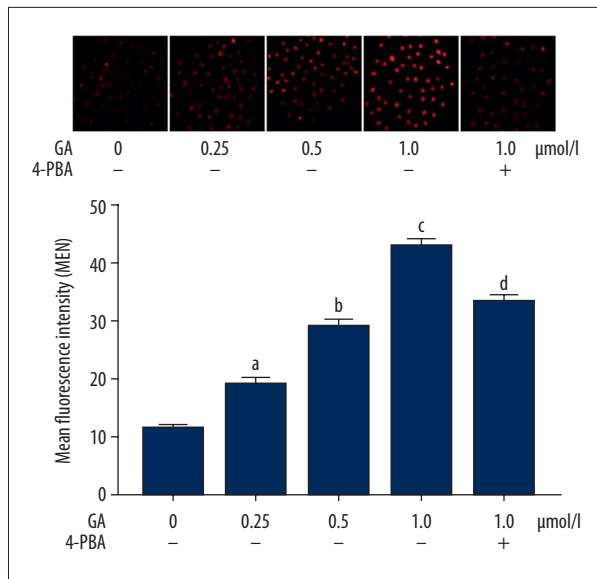


Figure 2. The upper panel demonstrates the captured images of DCFH-DA fluorescent staining of A549 cells incubated with gambogic acid (GA) at concentrations of 0, 0.25, 0.5, and 1.0 μmol/l. Generated intracellular ROS was tagged by red fluorescence. Columns on the lower panel indicate the detected mean fluorescence intensities (MFI) of DCFH-DA staining. [a Differences were statistically significant compared with control ($p < 0.05$); b Differences were statistically significant compared with cells incubated with GA at 0.25 μmol/l; c Differences were statistically significant compared with cells incubated with GA at 0.5 μmol/l; d Differences were statistically significant compared with cells incubated with GA at 1.0 μmol/l].

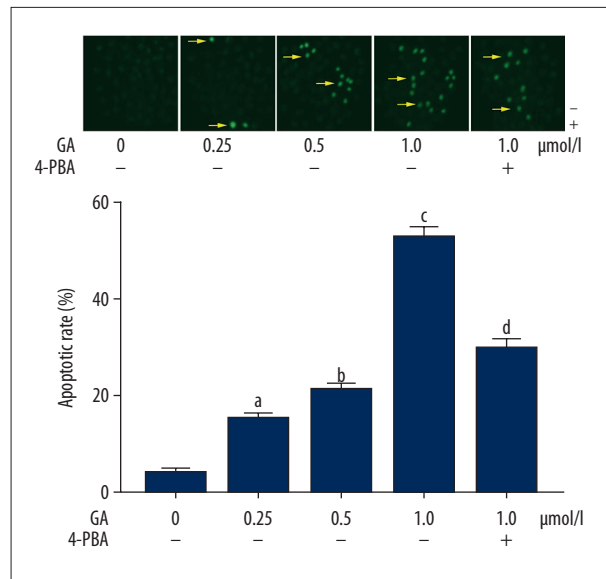


Figure 3. The upper panel demonstrates the captured images of TUNEL fluorescent staining of A549 cells incubated with gambogic acid (GA) at concentrations of 0, 0.25, 0.5, and 1.0 μmol/l. TUNEL-positive cells were tagged by green fluorescence, indicated by yellow arrows. Columns on the lower panel indicate the apoptotic rate of A549 cells. [a Differences were statistically significant compared with control ($p < 0.05$); b Differences were statistically significant compared with cells incubated with GA at 0.25 μmol/l; c Differences were statistically significant compared with cells incubated with GA at 0.5 μmol/l; d Differences were statistically significant compared with cells incubated with GA at 1.0 μmol/l].

was detected and measured by an inverted fluorescent microscope at 530 nm after being excited at 488 nm.

Cell apoptosis determination

Terminal transferase UTP nick-end labeling (TUNEL) assay was used to determine the apoptosis of NSCLC cells. Briefly, cells were incubated with 20 μmol/l proteinase K (Sigma) and then fixed by 4% paraformaldehyde (Solarbio). A TUNEL assay kit was applied to these cells to detect apoptosis according to the instructions provided by the manufacturer. The TUNEL-positive cells were detected and the images were captured by an inverted fluorescent microscope.

Western blot analysis

Cells were collected and suspended in a RIPA lysis buffer system (Santa Cruz) and whole-cell extract was prepared. Total protein was extracted using the Protein Extraction kit (Beyotime) according to the instructions provided by the manufacturer. A BCA kit (Beyotime) was used to measure the protein concentrations.

The protein was separated by vertical SDS-PAGE and then transferred to the PVDF membranes electronically. The blocking buffer (Santa Cruz) was applied to the membranes. Primary antibodies against GRP78 (1: 2000; Abcam), PERK (1: 2000; CST), p-PERK (1: 2000; CST), cleaved ATF6 (1: 2000; Abcam), IRE-1α (1: 4000; CST), p-IRE-1α (1: 2000; CST), CHOP (1: 2000; Abcam), caspase12 (1: 2000; Abcam), and GAPDH (1: 4000; Sigma) were used to incubate the membranes at 4°C for 8 h in TBST. Then, the corresponding secondary antibodies (Abcam) were used to incubate the membranes at room temperature for 1 h. The membranes were developed by an ECL kit (Pierce) and then exposed with the Gene Genius system (Syngene). The densities of the blots were then analyzed with Image J software.

Statistical analysis

Data are presented as mean ± SD. SPSS (ver. 16.0, SPSS) was used to analyze the data. Differences between groups were analyzed by one-way ANOVA, followed by Bonferroni post hoc analysis. The differences between groups were considered significant at $p < 0.05$.

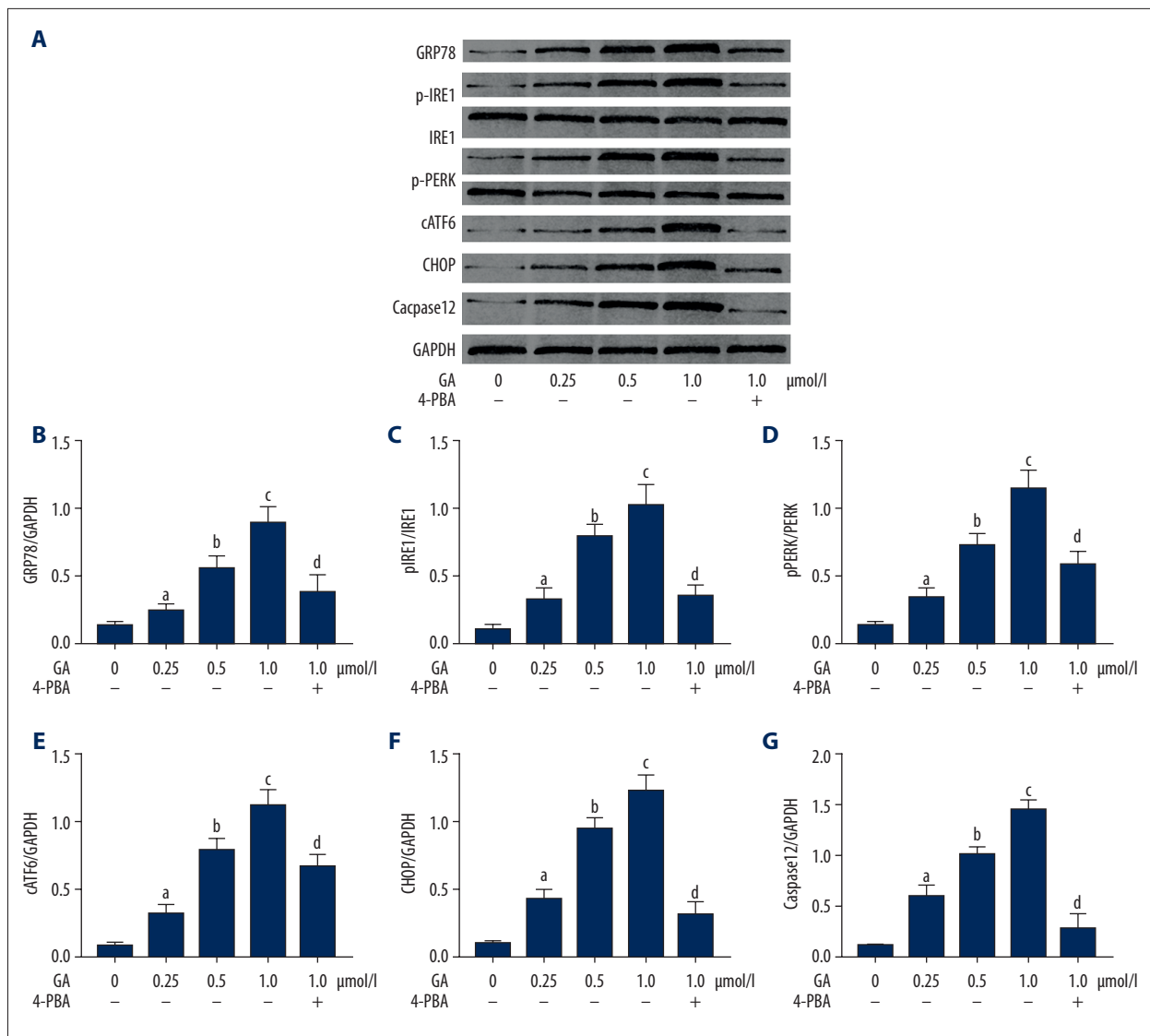


Figure 4. (A) Bands indicate the immunoblots of GRP78, p-IRE1, IRE1, p-PERK, PERK, cATF6, CHOP, caspase12, and GAPDH in A549 cells incubated with gambogic acid (GA) at concentrations of 0, 0.25, 0.5, and 1.0 $\mu\text{mol/l}$, respectively. (B) Columns indicate the relative expression level of GRP78 (normalized to GAPDH) in A549 cells. (C) Columns indicate the phosphorylation level of IRE1 (p-IRE1/IRE1) in A549 cells. (D) Columns indicate the phosphorylation level of PERK (p-PERK/PERK) in A549 cells. (E) Columns indicate the relative expression level of cATF6 (normalized to GAPDH) in A549 cells. (F) Relative expression level of CHOP (normalized to GAPDH) in A549 cells. (G) Relative expression level of caspase12 (normalized to GAPDH) in A549 cells. [^a Differences were statistically significant compared with control ($p < 0.05$); ^b Differences were statistically significant compared with cells incubated with GA at 0.25 $\mu\text{mol/l}$; ^c Differences were statistically significant compared with cells incubated with GA at 0.5 $\mu\text{mol/l}$; ^d Differences were statistically significant compared with cells incubated with GA at 1.0 $\mu\text{mol/l}$].

Results

GA incubation inhibited viability of NSCLC cells, which was impaired by 4-PBA (Figure 1). Compared with normal control, the GA incubation significantly reduced cell viabilities of A549 cells in a concentration-dependent manner ($P < 0.05$). However, co-treatment with 4PBA significantly impaired the inhibitory effects of GA on viability of NSCLC ($P < 0.05$).

GA treatment increased ROS production in NSCLC cells, which was impaired by 4-PBA. As demonstrated in Figure 2, the GA incubation increased the intracellular production of ROS in NSCLC cells in a concentration-dependent manner ($P < 0.05$). However, the co-administration of 4PBA reduced the ROS production in GA- incubated A549 cells ($P < 0.05$).

GA treatment increased apoptosis of NSCLC cells, which was impaired by 4-PBA (Figure 3). GA administration significantly

increased apoptosis of A549 cells in a concentration-dependent manner ($P < 0.05$). The co-administration of 4PBA, however, impaired the apoptosis-inducing effect of GA on NSCLC cells ($P < 0.05$).

GA treatment activated ERS and ERS-mediated apoptosis signaling, which was impaired by 4-PBA. As shown in Figure 4, the administration of GA significantly increased the expression levels of GRP78, cleaved ATF6, CHOP, and caspase12, as well as the phosphorylation levels of PERK and IRE1 α , in a concentration-dependent manner ($P < 0.05$). However, co-treatment with 4PBA reduced the expression levels of GRP78, cleaved ATF6, CHOP, and caspase12, as well as the phosphorylation levels of PERK and IRE1 α , in GA-incubated NSCLC cells ($P < 0.05$).

Discussion

The prognosis of NSCLC is poor when metastasis is identified [9,10]. Chemotherapy and radiotherapy are options, but their adverse effects limit use in some patients. Novel alternative anti-cancer agents have been attracting investigators' attention in recent decades [11]. In this study, we studied the anti-proliferative effect of GA on NSCLC cells, and we also performed an in-depth investigation of the possible involvement ER stress. We found that GA reduced viability of NSCLC cells via activating ROS-induced ER stress-mediated cell apoptosis.

In recent decades, many novel agents derived from natural medical herbs with potent anti-cancer effects have been identified and extracted or synthesized, and GA is one such promising agent [12]. Previous studies have reported that GA inhibits cell proliferation, invasion, and migration in many human cancers, including hepatic cancer, ovarian cancer, and gastric cancer [13,14]. In this study, human NSCLC cells were treated with GA at various concentrations. We found that the viability of NSCLC A549 cells was significantly inhibited by GA in an incubation-dependent and concentration-dependent manner. We also found that ER stress-induced apoptosis was involved in the anti-proliferative effects of GA on NSCLC cells.

As an important organelle, the ER has roles in many vital and fundamental cellular functions. The ER is believed to provide

the internal environment for protein folding and maturation in eukaryotic cells [15]. When facing prolonged and strong harmful stimuli, the ER induces a condition termed "ER stress" [16]. Sustained ER stress leads to activation of several ER stress-specific pro-apoptotic signaling pathways [16]. Correspondingly, the activation of PERK, IRE1 α , and ATF6 signaling eventually lead to activation of the pro-apoptotic factor CHOP, which facilitates activation of caspase12, causing caspase cascade activation [17]. In this study, our results showed that GA incubation significantly activated ER stress in a concentration-dependent manner, which was proved by the upregulation of GRP78, the molecular marker of ER stress. Correspondingly, the upregulation of ATF6, as well as the phosphorylation of IRE1 α and PERK, were found in GA-treated NSCLC cells. We also found that the ER stress-specific inhibitor 4-PBA significantly inhibited GA-induced apoptosis. We also found that 4-PBA suppressed GA-induced ER stress, and the activation of IRE1 α and PERK and ATF6 were also inhibited. These results support our suggestion that GA facilitates ER stress-induced apoptosis in NSCLC cells.

ROS are important intracellular mediators playing roles in maintaining normal cellular functions and causing cell injuries and cell death [18]. Many anti-cancer agents cause cell damage by generating excessive ROS [19]. Previous investigations suggested the role of ROS as one of the initiators of ER stress. Accumulated ROS induced unfolded and mis-folded protein production, which further induces ER stress [20]. In the present study, we found that GA treatment induced intracellular production of ROS in NSCLC cells. Massively accumulated intracellular ROS leads to ER dysfunction and thus induces ER stress. In the present study, we also found that the ER stress-specific agent 4-PBA alleviated apoptosis of GA-incubated NSCLC cells without dramatically affecting intracellular ROS levels. These results suggest that ROS are responsible for inducing ER stress-dependent apoptosis in GA-treated NSCLC cells.

Conclusions

According to the results of our study, we conclude that: 1) GA treatment reduced cell viability of NSCLC cells by inducing apoptosis; and 2) GA induced NSCLC cell death via ROS-induced ER stress-mediated pro-apoptotic signaling.

References:

1. Zheng H, Zhan Y, Liu S et al: The roles of tumor-derived exosomes in non-small cell lung cancer and their clinical implications. *J Exp Clin Cancer Res*, 2018; 37: 226
2. Ying J, Zhang M, Qiu X, Lu Y: The potential of herb medicines in the treatment of esophageal cancer. *Biomed Pharmacother*, 2018; 103: 381-90
3. Banik K, Harsha C, Bordoloi D et al: Therapeutic potential of gambogic acid, a caged xanthone, to target cancer. *Cancer Lett*, 2018; 416: 75-86
4. Yan X, Yang Y, He L et al: Gambogic acid grafted low molecular weight heparin micelles for targeted treatment in a hepatocellular carcinoma model with an enhanced anti-angiogenesis effect. *Int J Pharm*, 2017; 522: 110-18
5. Tang Q, Lu M, Zhou H et al: Gambogic acid inhibits the growth of ovarian cancer tumors by regulating p65 activity. *Oncol Lett*, 2017; 13: 384-88
6. Wang Y, Liang X, Tong R et al: Gambogic acid-loaded polymeric micelles for improved therapeutic effect in breast cancer. *J Biomed Nanotechnol*, 2018; 14: 1695-704

7. Verfaillie T, Garg AD, Agostinis P: Targeting ER stress-induced apoptosis and inflammation in cancer. *Cancer Lett*, 2013; 332: 249–64
8. Li Y, Guo Y, Tang J et al: New insights into the roles of CHOP-induced apoptosis in ER stress. *Acta Biochim Biophys Sin*, 2014; 46: 629–40
9. Zhang Y, Yang Q, Wang S: MicroRNAs: A new key in lung cancer. *Cancer Chemother Pharmacol*, 2014; 74: 1105–11
10. Albano D, Bilfinger T, Nemesure B: 1-, 3-, and 5-year survival among early-stage lung cancer patients treated with lobectomy vs. SBRT. *Lung Cancer (Auckland, NZ)*, 2018; 9: 65–71
11. Fan XX, Pan HD, Li Y et al: Novel therapeutic strategy for cancer and autoimmune conditions: Modulating cell metabolism and redox capacity. *Pharmacol Ther*, 2018; 191: 148–61
12. Youns M, ElKhoely A, Kamel R: The growth inhibitory effect of gambogic acid on pancreatic cancer cells. *Naunyn Schmiedebergs Arch Pharmacol*, 2018; 391(5): 551–60
13. Yin D, Yang Y, Cai H et al: Gambogic acid-loaded electrosprayed particles for site-specific treatment of hepatocellular carcinoma. *Mol Pharm*, 2014; 11: 4107–17
14. Zou ZY, Wei J, Li XL et al: Enhancement of anticancer efficacy of chemotherapeutics by gambogic acid against gastric cancer cells. *Cancer Biother Radiopharm*, 2012; 27: 299–306
15. Liu ZW, Zhu HT, Chen KL et al: Protein kinase RNA-like endoplasmic reticulum kinase (PERK) signaling pathway plays a major role in reactive oxygen species (ROS)-mediated endoplasmic reticulum stress-induced apoptosis in diabetic cardiomyopathy. *Cardiovasc Diabetol*, 2013; 12: 158
16. McGrath EP, Logue SE: The unfolded protein response in breast cancer. *Cancers (Basel)*, 2018; 10(10): pii: E344
17. Chiu TL, Su CC: Tanshinone IIA increases protein expression levels of PERK, ATF6, IRE1alpha, CHOP, caspase3 and caspase12 in pancreatic cancer BxPC3 cell-derived xenograft tumors. *Mol Med Rep*, 2017; 15: 3259–63
18. Verfaillie T, Rubio N, Garg AD et al: PERK is required at the ER-mitochondrial contact sites to convey apoptosis after ROS-based ER stress. *Cell Death Differ*, 2012; 19: 1880–91
19. Shan S, Shi J, Li Z et al: Targeted anti-colon cancer activities of a millet bran-derived peroxidase were mediated by elevated ROS generation. *Food Funct*, 2015; 6: 2331–38
20. Chang CW, Chen YS, Tsay YG et al: ROS-independent ER stress-mediated NRF2 activation promotes Warburg effect to maintain stemness-associated properties of cancer-initiating cells. *Cell Death Differ*, 2018; 9: 194